



Fundamental Limits to Nonlinear Energy Harvesting

Ashkan Haji Hosseinloo* and Konstantin Turitsyn

*Department of Mechanical Engineering, Massachusetts Institute of Technology,
77 Massachusetts Avenue, Cambridge, Massachusetts 02139, USA*

(Received 24 December 2014; revised manuscript received 28 October 2015; published 29 December 2015)

Linear and nonlinear vibration energy harvesting has been the focus of considerable research in recent years. However, fundamental limits on the harvestable energy of a harvester subjected to an arbitrary excitation force and different constraints is not yet fully understood. Understanding these limits is not only essential for an assessment of the technology potential, but it also provides a broader perspective on the current harvesting mechanisms and guidance in their improvement. Here, we derive the fundamental limits on the output power of an ideal energy harvester for arbitrary excitation waveforms and build on the current analysis framework for the simple computation of this limit for more sophisticated setups. We show that the optimal harvester maximizes the harvested energy through a mechanical analog of a buy-low-sell-high strategy. We also propose a nonresonant passive latch-assisted harvester to realize this strategy for an effective harvesting. It is shown that the proposed harvester harvests energy more effectively than its linear and bistable counterparts over a wider range of excitation frequencies and amplitudes. The buy-low-sell-high strategy also reveals why the conventional bistable harvester works well at low-frequency excitation.

DOI: [10.1103/PhysRevApplied.4.064009](https://doi.org/10.1103/PhysRevApplied.4.064009)

I. INTRODUCTION

The problem of energy supply is one of the biggest issues in miniaturizing electronic devices. Advances in technology have reduced the power consumption in electronic devices such as wireless sensors, data transmitters, and medical implants to the point where ambient vibration, a universal and widely available source of energy, has become a viable alternative to costly traditional batteries. A typical vibratory energy harvester (VEH) consists of a vibrating host structure, a transducer (e.g., electromagnetic, electrostatic, or piezoelectric), and a harvesting circuitry (e.g., a simple electrical load).

Most of the conventional VEHs exploit linear resonance, i.e., tuning the natural frequency of the host structure to the excitation frequency, to maximize the harvested energy. This approach has three obvious downsides: an inherent narrow bandwidth of linear resonance and limited robustness, an inefficiency in real-world applications with wideband and nonstationary excitation sources, and the big gap between the low frequency of the typical excitation sources (such as waves and walking motion), and the high natural frequency of small-scale linear VEHs. In fact, nonstationary and random vibration are more common than harmonic excitation in many practical applications [1–4]. To overcome these limitations, researchers have recently tried to make use of the purposeful introduction of nonlinearity in VEH design [5]. One of the key challenges in designing nonlinear harvesters is the immense range of possible nonlinearities. Among

different types of nonlinearity, bistability has received more attention in the past few years [6–10]. However, the question of what are the fundamental limitations of nonlinear energy harvesting is still open.

The explicit identification of fundamental performance limits has played a crucial role in many fields of science and engineering. In the energy field, the classical Carnot cycle efficiency was a guiding principle for the development of thermal power plants and combustion engines. It has also inspired scientific debates that consequently lead to the formation of modern statistical physics. The Lanchester-Betz limit for wind harvesting efficiency [11], and the Shockley-Queisser limit for the efficiency of solar cells [12] are commonly used for the long-term assessment of sustainable energy policies. Shannon's limit of information capacity [13] has formed a foundation for the development of modern communication systems. The Bode's-sensitivity-integral limits in feedback control theory [14] provide a standard tool for the analysis of design trade-offs in modern control systems.

There have been very few, but influential, studies in the context of energy harvesting that have addressed the question of the maximal power limits for VEHs. The idea of maximizing the harvested energy was originated in the seminal works by Mitcheson *et al.* [15,16] and Ramlan *et al.* [17]. Mitcheson *et al.* [15] derived the maximum harvested power for velocity-damped and Coulomb-damped resonant generators as well as for the Coulomb-force parametric generator (CFPG) with one mechanical degree of freedom when subjected to harmonic excitation. They also estimated the maximum possible harvested power for a general harvesting device excited by harmonic

*Corresponding author.
ashkanhh@mit.edu

force using proof mass traversal at the force extrema [16]. Ramlan *et al.* [17] took an energy approach and estimated the available power from a nonlinear VEH subjected to harmonic excitation. They showed that with a displacement constraint, the nonlinear harvester can harvest in the limit of $4/\pi$ times what a tuned linear VEH can harvest.

More recently, similar to Ref. [17] but in a more advanced fashion, Halvorsen *et al.* [18] derived upper bound limits for a harvester with one mechanical degree of freedom and linear damping. They considered arbitrary general excitation waveforms in the absence of displacement limits (damping-dominated motion) and periodic excitation with displacement limits. The upper bound limit for a damping-dominated motion was generalized to multiple sinusoid input by Heit and Roundy [19]. Also, the maximal power limits for nonlinear energy harvesters under white-noise excitation were explored in Refs. [20–22]. Although these studies address the same fundamental question, the white-noise approximation is rather restrictive and leads to overly conservative bounds. This assumption may not be applicable to many practical settings where most of the energy-harvesting potential is associated with low frequencies.

Although the question of fundamental limits to the energy conversion rate in the context of the vibratory energy harvesters has received limited attention thus far, these types of questions have been studied much more thoroughly in statistical physics. For example, the seminal Jarzynski relation derived in Ref. [23] can be interpreted as the statistical constraint on the possible efficiency of the work to the free energy conversion process. More general relations have been derived in Refs. [24,25] for entropy production in stochastic systems. The stochastic systems appearing in vibratory system analysis are specific examples of the so-called nonequilibrium steady states that were studied, for example, in Refs. [25,26]. Despite the immense effort in the statistical physics community, most of the studies have focused on the systems where the stochastic fluctuations have a thermal nature and satisfy special fluctuation-dissipation relations. This is the case in many practically relevant systems, such as molecular motors [27] or optical trap experiments [28]. The main challenge with the extension of these results to the vibrational systems is the inherent nonequilibrium nature of the fluctuations that requires more general approaches not relying on underlying microscopic statistical features of the system. However, more general approaches relying on the techniques from control and information theory [29] may eventually lead to the convergence of these currently separate fields.

In this study, we build on the current framework for deriving the energy-harvesting limits, generalize it to almost arbitrary excitation waveforms, and provide insights into how to approach these limits in practice. To illustrate the approach, we build a hierarchy of increasingly more constrained models of nonlinear harvesters, derive the

closed-form solutions for simplest models, and provide general formulations where the closed-form solutions do not exist. Inspired by the optimal solutions to the simple model, we propose a conceptual design of nonresonant latch-assisted (LA) nonlinear harvesters and show that they are significantly more effective than the traditional linear and nonlinear harvesters in broadband low-frequency excitation that is common to practical situations.

II. IDEAL ENERGY HARVESTING

We consider a model of a single-degree-of-freedom ideal energy harvester characterized by the mass m and the displacement $x(t)$ that is subjected to the energy-harvesting force $f(t)$ and exogenous excitation force $F(t)$. The dynamic equation of the system is a Newton's second law $m\ddot{x}(t) = F(t) + f(t)$. The fluxes of energy in the system are given by the expressions $F\dot{x}$, $-f\dot{x}$, and $(m/2)\dot{x}^2$ representing, respectively, the external input power to the system, harvested power, and instantaneous kinetic energy of the system.

We start our analysis by considering an idealized harvester with no constraints imposed on either the harvesting force $f(t)$ or the displacement $x(t)$. It is easy to show that the overall harvesting rate in this setting is unbounded. Indeed, the trajectory defined by a simple relation $\dot{x}(t) = \kappa F(t)$ that can be realized with the harvesting force $f = m\kappa\dot{F} - F$ results in the harvesting rate of κF^2 that can be made arbitrarily large by increasing the mobility constant κ . This trivial observation illustrates that the question of fundamental limits is well posed only for the model that incorporates some technological or physical constraints. This is a general observation that applies to most of the known fundamental limits. For example, the Carnot cycle limits the efficiency of cycles with bounded working fluid temperature, and the Shannon capacity defines the limits for signals with bounded amplitudes and bandwidth.

To derive the first nontrivial limits to the energy-harvesting power limits we consider the displacement amplitude and energy dissipation constraints that are common to all energy harvesters. For the first constrained model we consider the displacement constraint with the trajectory limited in a symmetric fashion, i.e., $|x(t)| \leq x_{\max}$, where x_{\max} is the displacement limit. In this model we assume there is no natural dissipation of energy in the system, so in the steady state motion, the integral net input of energy into the system equals the harvested energy. Thus, the maximum harvested energy could be evaluated simply by maximizing the following expression [18]:

$$E_{\max} = \max_{x(t)} \int dt F(t) \dot{x}(t). \quad (1)$$

Here, the optimization is carried over the set of all “reachable” trajectories, that can be realized given the system constraints. As long as the harvesting force f is not subjected to any constraints, this set simply coincides with

the set of bounded trajectories defined by $|x(t)| \leq x_{\max}$. The optimal trajectory is then easily found by rewriting the integral in Eq. (1) as $-\int dt \dot{F}(t)x(t)$. It is straightforward to check that this expression is maximized by

$$x_*(t) = -x_{\max} \text{sign}[\dot{F}(t)]. \quad (2)$$

The interpretation of Eq. (2) is straightforward and can be summarized as a buy-low-sell-high (BLSH) harvesting strategy. The optimal harvester keeps the mass at its lowest (highest) position until the force F reaches its local maximum (minimum) and then activates the force f to move the mass by $2x_{\max}$ upwards (downwards) as fast as possible. In general, f is not passive for all time, and this mechanism is in fact nonresonant. Similar results were reported for time harmonic excitation in Ref. [18]. Also, the CFPG discussed in Ref. [15] follows a similar displacement trajectory as Eq. (2) when the excitation is harmonic with a relatively large force amplitude. However, if the excitation is nonstationary or not harmonic the trajectories will be very different and CFPG will not track the changes in the direction of the external forcing $F(t)$, unlike BLSH described by Eq. (2).

The BLSH strategy is remarkably similar to the strategy employed by the Carnot cycle machine and can also be derived using similar geometric arguments. In the F - x parametric plane, the overall harvested energy is defined as the integral $\oint F dx$ representing the area of the contour produced by the cycle. For a local realization of the force, both the values of the force and the values of displacement are bounded, so the energy is maximized by the contour with a rectangular shape. Similarly, the Carnot cycle has a simple rectangular shape in the temperature-entropy T - S diagram derived by recognizing that the overall work given by $\oint T dS$ is the area of the contour that is constrained by the temperature limits.

The net harvested energy in this model can be expressed as $E_{\max} = x_{\max} \int |\dot{F}(t)| dt$. For commonly used Gaussian models of the random external forces characterized by the Fourier transform $F_{\omega} = \int dt \exp(i\omega t) F(t)$, and corresponding power spectral density $|F_{\omega}|^2$, the quantity $\dot{F}(t)$ is a Gaussian random variable with zero mean and the variance given $\int (d\omega/2\pi) \omega^2 |F_{\omega}|^2$. Therefore, the maximal harvesting energy is given by the following simple expression:

$$E_{\max} = x_{\max} \frac{2}{\pi} \sqrt{\int \frac{d\omega}{2\pi} \omega^2 |F_{\omega}|^2}. \quad (3)$$

The strategy favors the high frequency harmonics which produce frequent extrema of the external force, each coming with the harvesting opportunity. In practice, harvesting energy at very high harmonics will not work because of the natural energy dissipation in the system. So, in our next model, we consider the limits associated with dissipation.

To make the analysis tractable we define another model without the displacement constraints (so $x_{\max} = \infty$), but with the additional damping force $F_d = -c_m \dot{x}$. Consequently, the dynamic equation changes to $m\ddot{x}(t) + c_m \dot{x}(t) = F(t) + f(t)$, and $c_m \dot{x}^2(t)$ represents the power dissipated in the mechanical damper. The harvested energy $-\int dt f(t)\dot{x}(t)$ is then equal to $\int dt [F(t)\dot{x}(t) - c_m \dot{x}^2(t)]$, assuming no accumulation of energy in the system at steady state. This is a simple quadratic function in \dot{x} that is maximized by $\dot{x} = F/2c_m$, thus resulting in the following integral energy expression.

$$E_{\max} = \max \int dt [F(t)\dot{x} - c_m \dot{x}^2] = \int \frac{F^2(t)}{4c_m} dt. \quad (4)$$

As in the previous models, without any constraints on the harvesting force, the trajectory is achievable with the input harvesting force of the form $f(t) = m\ddot{x}_*(t) - F(t)/2$. These results were also reported by Halvorsen *et al.* [18]. Furthermore, using Parseval's theorem and the final result in Eq. (4), the maximum energy in the frequency domain is equal to $E_{\max} = \int (d\omega/8\pi c_m) |F_{\omega}|^2$. This simple frequency-domain representation has an important property that with the optimal and ideal harvester force, the energy is harvested from all the frequency components of the excitation force equally proportionate to the power spectrum of the forcing function. This is very advantageous to low frequency and broadband vibration sources such as wave or walking motion, where efficient resonant harvesting is not possible.

In a similar fashion, it is possible to construct more complicated limits that combine multiple constraints. Although most of these models do not admit a closed-form solution, the corresponding optimization problem can be transformed into a system of differential algebraic equations (DAEs) using the Lagrangian multiplier and slack variable techniques. For example, the incorporation of the displacement constraints into a damped harvesting model can be accomplished by solving the following variational problem:

$$E_{\max} = \max \int dt [F\dot{x} - c_m \dot{x}^2 - \mu \mathcal{E} - \lambda (\mathcal{I} - \alpha^2)]. \quad (5)$$

Here, the unconstrained optimization is carried over $x(t)$, $f(t)$, the two Lagrangian multiplier functions $\lambda(t)$ and $\mu(t)$, and the so-called slack variable $\alpha(t)$. The function $\mathcal{E}(x, \dot{x}, \ddot{x}, t) = m\ddot{x} + c_m \dot{x} - F - f$ represents the equality constraint associated with the equations of motion, while the indicator function $\mathcal{I}(x) = x_{\max}^2 - x^2$ that is positive only on an admissible domain represents the inequality constraint for the displacement. Other equality and inequality constraints on the displacement, velocity, or harvesting force can be naturally incorporated in a similar way. Using the standard Euler-Lagrangian variational approach the

problem can be transformed into a system of DAEs that can be solved for arbitrary forcing functions and thus provide universal benchmarks for any practical harvesters.

It is worth noting that the general approach of studying the extremal behavior of the physical systems using the variational approach is by no means new. In its modern form it originated in the quantum field theory [30] but has since been applied in many fields, most notably in one of the most difficult nonlinear problems of turbulent dynamics [31]. Halvorsen *et al.* [18] also used a similar variational approach to find the maximal power bound for a VEH subjected to period excitation and displacement limits.

The innocent-looking DAEs that resulted from applying the variational approach to the Lagrangian in Eq. (5) are not always easy to solve even computationally (particularly if the DAEs have a high index). However, the time-discretized objective function in Eq. (4) can be maximized using standard nonlinear optimization approaches. In particular, the optimization of quadratic functionals like Eq. (4) complemented by any linear equality and inequality constraints like $m\ddot{x} = F + f$ and $|x| < x_{\max}$ can be easily performed using standard convex optimization techniques [32]. Discretization of the system can be accomplished by using the spectral representation of the force and displacement signals.

To illustrate the generality and efficacy of this approach in handling different practical constraints and complexities, we attempt to find the power bounds of the same system described above (with mechanical dissipation) with some additional constraints. First, we apply dissipativity constraint on the harvesting force f , i.e., $f\dot{x} \leq 0$, that prevents the injection of positive energy from the controller. Second, we assume the nonideal actuator, with losses $-df^2 - ef^2$ related to actuation force generation. Typically those are resistive Ohmic losses due to currents required

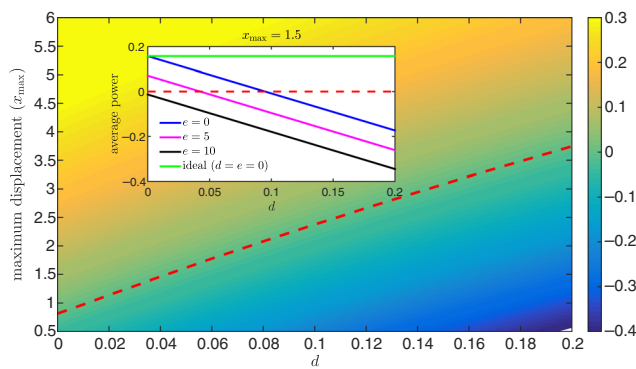


FIG. 1. Contour plot of optimal average harvested power with penalty coefficient $e = 5$ as a function of penalty coefficient d and displacement limit x_{\max} when subjected to harmonic excitation $F(t) = 2 \sin(0.1t)$. The numerical values of $m = 1$ and $c_m = 1$ are used. The dashed red line shows the transition from the potentially harvestable regime to the nonharvestable regime. The inset shows the optimal average power in terms of d for different values of e for a fixed displacement limit of $x_{\max} = 1.5$.

for electromagnetic or electrostatic force f generation. Optimization results are reflected in Fig. 1. The figure reveals the transition from the regime where energy could potentially be harvested to the regime where no energy could be harvested no matter how the system is optimized or designed. This is an unexpected consequence of the $|x| \leq x_{\max}$ constraint, as one can easily see that harvesting is always possible in linear systems.

III. FORCE CONSTRAINTS

A small-scale harvester with an ideal arbitrary harvesting force may not be easily realizable with the current technology. More accurate power limits can be derived on models incorporating additional constraints on the harvesting force $f(t)$. In a more realistic representation of the system, the harvesting force $f(t)$ can be decomposed into three parts. First, there is an inherent or intentionally introduced restoring force from the potential energy $U(x)$ usually originating from the mechanical strain of a deflected cantilever harvester or a magnetic field. Second, there is the linear harvesting energy force $c_e \dot{x}$ that is typical to most of the traditional conversion mechanisms, particularly to electromagnetic transduction mechanisms. Finally, controlled harvesters may also utilize an additional control force $u(t)$ to enhance the energy-harvesting effectiveness. The control force cannot be used for direct extraction of energy from the system, however, it can be used to change the dynamics of the system in a way that increases the overall conversion rate $c_e \dot{x}^2$. More precisely, the overall energy harvested from the system is given by $\int dt [c_e \dot{x}^2 - w(t)]$, where $w(t)$ represents the power necessary to produce the control force $u(t)$ and its corresponding power $p(t) = u(t)\dot{x}$. The power flows in the system are illustrated schematically in Fig. 2. The corresponding optimization problem can be written as

$$E_{\max} = \max \int dt [F\dot{x} - c_m \dot{x}^2 - l(t)]. \quad (6)$$

Here, the new function $l(t) = w(t) - p(t)$ represents the losses of power during the control process. The specifics of the losses process depend on the details of the system

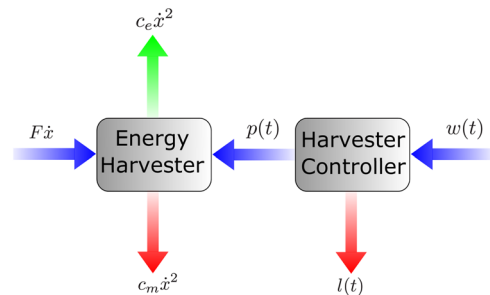


FIG. 2. Power flow diagram of the VEH consisting of the main harvesting system coupled with its harvesting controller.

design and can be difficult to analyze in a general setting. However, it is easy to incorporate a number of common natural and technological constraints on the loss rate. First, the second law of thermodynamics implies that the losses are always positive. If the control system cannot accumulate any energy, this constraint can be represented simply as $l(t) \geq 0$. If energy accumulation is possible, only the integral constraint can be enforced: $\int l(t)dt \geq 0$. Obviously, if the former is the only constraint imposed on the system, the optimal solution would correspond to zero losses $l = 0$ and it coincides with previous analysis of an ideal harvester.

More interesting bounds can be obtained by incorporating common technological constraints. The obvious one is introducing limits on the force value $u_{\min} \leq u(t) \leq u_{\max}$ that can be naturally added via additional slack variables as described above or as the bounds on the decision variables if one chooses to do the discrete nonlinear optimization approach. The other two constraints represent different levels of sophistication of the harvesting control system. First is the inability of the control system to harvest the energy. Typically, the conversion of mechanical energy to a useful electrical one happens only through the electric damping mechanism characterized by the force $c_e \dot{x}$. In this case, the work done to produce the control input is constrained to be positive, so $w(t) \geq 0$ or $l(t) \geq -u\dot{x}$. This setup corresponds to a harvesting system where the control force $u(t)$ can inject the energy (positive and/or negative) into the system but cannot harvest it from the system. An even more restrictive constraint would correspond to a situation where the control system cannot inject positive energy at all. This type of control is only capable of increasing the natural dissipation rate, thus acting as an effective break. In this case, the power injection can be only negative, i.e., dissipative, so $u(t)\dot{x} \leq 0$.

These two extensions of the problem can be naturally transformed either into nonlinear systems of DAEs using the slack variable technique explained above or into a nonlinear and hopefully convex optimization problem after discretization in time. Numerical analysis of these equations may provide upper bounds on the harvested energy limits. Comparison of different bounds would then provide a natural way of valuing the potential benefits of possible control systems used in energy harvesters.

IV. NONRESONANT LATCH-ASSISTED ENERGY HARVESTING

To further illustrate the usefulness of the harvesting power limits, we propose a novel nonlinear and nonresonant harvester that is inspired by the behavior of an ideal harvester with no mechanical damping described by Eq. (2). The harvester is based on a simple extension of a classical linear mass-spring-damper system with a simple latch mechanism that can controllably keep the system

close to $x = \pm x_{\max}$ positions mimicking the ideal harvester and to enforce the trajectory expressed by Eq. (2).

More specifically, we use a simple control strategy where the secondary stiff spring representing the latch is activated when the harvester mass reaches its maximum or minimum displacement limit. The harvester mass is held at the limit after this activation. When the force reaches its extremal value a signal is sent to the latch mechanism to release the mass by detaching the secondary spring. The dynamic equation of this system could be rewritten as $m\ddot{x}(t) + (c_m + c_e)\dot{x}(t) + U_0'(x) = F(t) - U_l'(x)\sigma(t)$, where $\sigma(t)$ is the signal for activation or deactivation of the latch system. $U_0(x)$ and $U_l(x)$ are, respectively, the potential energy of the harvester's linear restoring force and the latch mechanism. Signal generation of $\sigma(t)$ may practically require a minimal energy, but otherwise the LA harvester is completely passive.

Figure 3 illustrates the concept of maximizing the harvested energy through a latch mechanism as one method to mimic the trajectory in Eq. (2). In this method, almost all of the work is done on the system when the system is moving from one end to the other; this energy is then harvested and dissipated when the system is blocked by a latch from moving outside of the extremal points. Whenever the excitation is slow in comparison to the natural period of the harvester, the system translates between the extrema very quickly, while the force remains close to its extremal values. The system takes natural advantage of the frequencies, and, unlike traditional linear harvesters, has a higher effectiveness at low frequencies.

Figures 4(a) and 4(b) depict displacement and energy time histories, respectively, for LA, linear, and bistable harvesters subjected to harmonic excitation. The most common bistable potential is used here for comparison. The bistable potential is of the quartic form $U(x) = -a(x^2/2 - x^4/4x_s^2)$, where $a = 5$ and $x_s = 0.875$ (stable

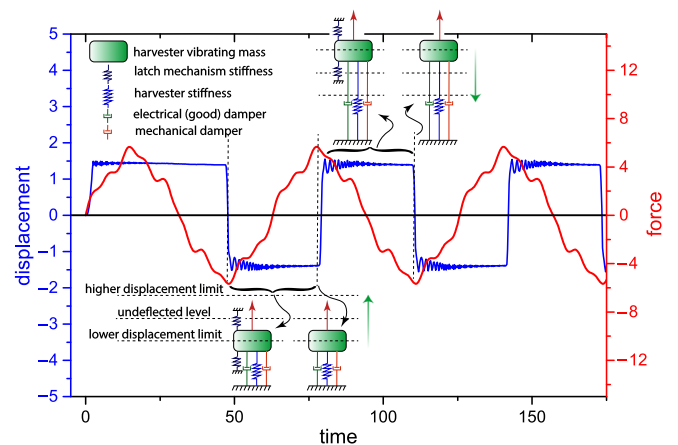


FIG. 3. *Latch-assisted harvester.* Here, an energy harvester with linear mechanical and electrical damping and linear stiffness is considered. Vibration travel is constrained to 1.5 units, i.e., $|x(t)| \leq 1.5$.

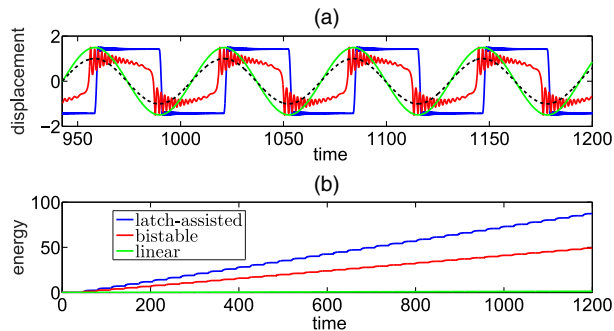


FIG. 4. *Displacement and energy time histories.* (a) The displacement time history for the three linear, bistable, and latch-assisted harvesters. Damping ratios of $\zeta_m = 0.02$ and $\zeta_e = 0.1$, and a displacement limit of 1.5 units are used. The excitation is harmonic of the form $F(t) = 2 \sin(0.1t)$ and its scaled waveform (scaled to unity in amplitude) is plotted as a dashed line. (b) The corresponding energy time history for the three harvesters.

equilibrium) are the tuning parameters. For a fair comparison the bistable and linear systems are first optimized for a given force statistics and displacement constraints. Also, all the variables in all of the figures are dimensionless. Dimensionless energy is calculated by evaluating $\int_0^t \zeta_e \dot{x}(t')^2 dt'$. It could be seen from the figure that energy is transferred to the LA harvester mainly when the mass is allowed to move from one displacement limit to the other, and the energy is harvested during this period and after this period when the harvester mass is held at one end. It could also be seen that at low frequencies the bistable harvester tries to mimic the LA harvester by keeping the mass at one end in one of its wells and releasing it at a later time close to the extremum of the excitation force. This is a very important insight as to why and how the bistable harvester works better than the linear one, particularly at low frequencies.

Figure 5 gives further insight into the origin of high energy-harvesting effectiveness of the latch-assisted mechanism. We plot phase diagrams for the LA harvester as well as for linear and bistable harvesters in Fig. 5(a). According to Fig. 5(a), the translation between the two ends occurs at the greatest speed in the latch-assisted harvester that could be indicative of better energy harvesting. Figure 5(b) is even more illustrative, showing the force capable of doing positive work versus displacement. In this figure, the ideal harvester has a perfect rectangle curve, analogous to the perfect rectangle of the Carnot engine in the T - S diagram. All other harvesters fall inside this rectangle enclosing a smaller area.

To check the robustness and compare the efficient-harvesting range, the performance of the three harvesters over a wide range of base-excitation frequencies and amplitudes is illustrated in Fig. 6. In this experiment, fixed parameters are used for all three harvesters for the full range of excitation statistics (e.g., $a = 0.5$ and $x_s = 1$ for

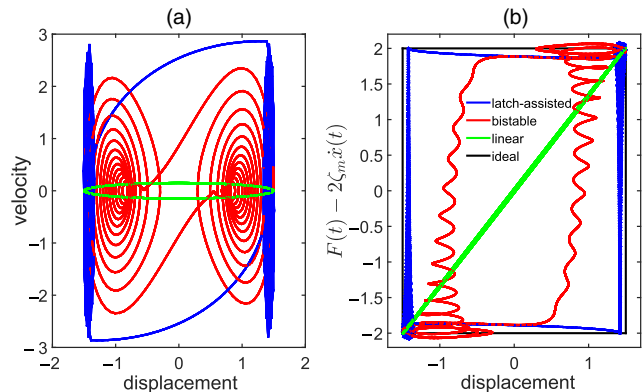


FIG. 5. *Phase and force-displacement diagrams.* (a) The phase diagram for the three linear, bistable, and latch-assisted systems. Damping ratios of $\zeta_m = 0.02$ and $\zeta_e = 0.1$ and a displacement limit of 1.5 units are used. The excitation is harmonic of the form $F(t) = 2 \sin(0.1t)$. (b) The force-displacement curves for the linear, bistable, latch-assisted mechanism, and ideal harvester with no mechanical damping.

the bistable system). To make sure that the harvesters are confined within the displacement limit (2.5 units in this case), very stiff walls at $\pm x_{\max}$ are implemented in the simulations. The latch-assisted harvester has a higher power over a wider range of excitation frequencies and amplitudes. The LA harvester works best at low frequencies and large amplitudes where it can mimic the ideal harvester best. The low effectiveness of the LA harvester at low frequencies and small amplitudes is because the system does not reach the displacement limits to latch, and hence works like a linear system in this region.

It has been shown that the current nonlinear harvesters, in particular, the bistable harvesters, are sensitive to the type of excitation, and may not be very effective when subjected to real ambient vibration sources [33]. To analyze how robust and efficient the LA harvester is when subjected to real-world vibration signals, we tested its performance on real experimental data of walking motion at the hip level [34] which is inherently a low-frequency motion. According to Fig. 7, the latch-assisted system outperforms the other two systems.

Implementation is also an important aspect of theoretical studies that should be addressed. Common nonlinear VEHs have been experimentally tested in recent years (see, e.g., Refs. [35–37]). The CFPG setup [15] with an adjusted logic could be used to implement the BLSH strategy. Another way to implement the LA VEH could be through an *adaptive* bistable system with time-dependent values of a and x_s used to hold and release the mass at proper times. To do so and mimic the LA mechanism, the adaptive bistable system should create a huge potential barrier when the harvester mass reaches the displacement limits (stable wells) and then kill the barrier when the harvester mass is supposed to traverse between the displacement limits based

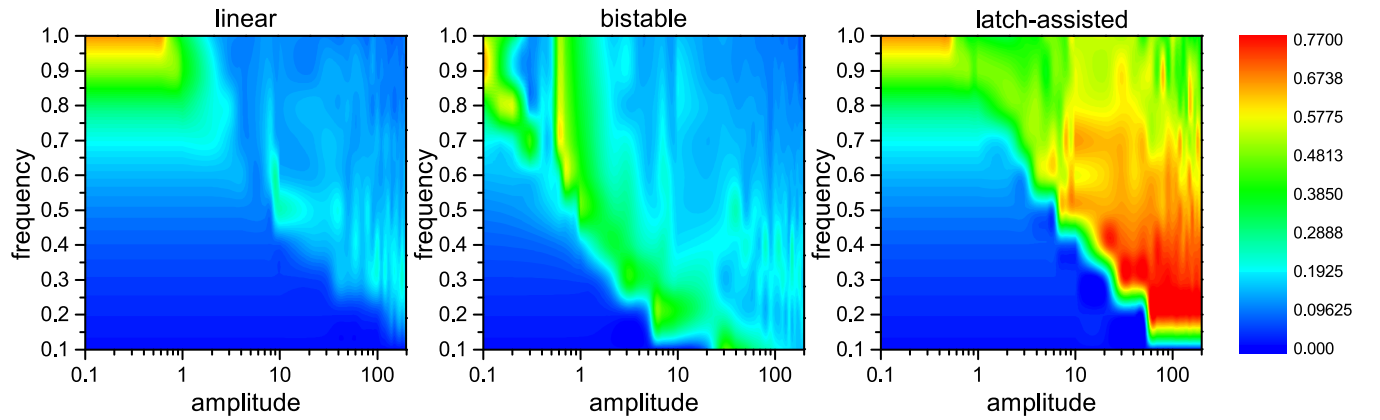


FIG. 6. *Normalized average harvested power contours.* The normalized average power of the three harvesters for a wide range of harmonic base-excitation amplitude and frequency is plotted for a fixed displacement limit of 2.5 units. The average power is normalized by the maximum average power that could be harvested by an ideal harvester with no mechanical damping.

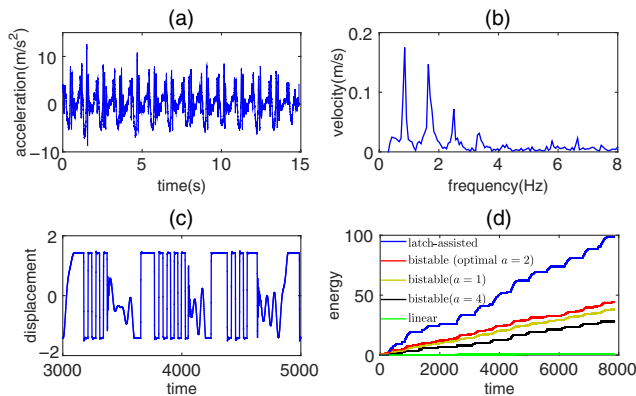


FIG. 7. *Energy harvesting while walking.* (a) Time history and (b) velocity spectrum of experimental acceleration recorded at the hip while walking [34]. (c) Displacement time history of the nonlinear LA VEH when base excited by walking motion. Displacement and time (frequency) are scaled by $13 \mu\text{m}$ and 500 rad/s , respectively. The same damping ratios and displacement limit of 1.5 units are used. (d) Time history of nondimensional harvested energy for the three systems. In addition to the optimal bistable harvester ($x_s = 0.9$ and $a = 2$), the performance of two bistable harvesters with detuned parameter a is also illustrated.

on the BLSH logic. It is worth mentioning that this is a completely passive process.

V. CONCLUSION

In conclusion, we have generalized and extended the current analysis framework and model hierarchy for the derivation of fundamental limits of the nonlinear energy-harvesting rate. The framework allows an easy incorporation of almost any constraints and arbitrary forcing statistics and represents the maximal harvesting rate as a solution of either a set of DAEs or a standard nonlinear optimization problem. Closed-form expressions were derived for two cases of harvesters constrained by

mechanical damping (damping-dominated motion) and maximal displacement limits. The results for damping-dominated motion were already reported in Ref. [18] but were derived here for the sake of completeness and also to add a few more comments on it. For the more practical and interesting constraint, i.e., the displacement constraint, we showed that a universal *buy-low-sell-high* logic guarantees a maximum harvested energy when there is no or very small mechanical damping. To illustrate the value of the limits and this logic, we have proposed a simple concept for nonlinear energy harvesting that mimics the performance of the optimal system using a passive and nonresonant latch mechanism. The proposed mechanism outperforms both linear and bistable harvesters in a wide range of parameters including the most interesting regime of low-frequency large-amplitude excitation where the current harvesters fail to achieve high performance. It was also shown that the conventional bistable harvester tries to mimic the BLSH logic at low frequencies, which provides a conceptual insight into why and how the bistable harvester performs well at low excitation frequencies.

- [1] A. H. Hosseinloo, F. F. Yap, and E. T. Chua, Random vibration protection of a double-chamber submerged jet impingement cooling system: A continuous model, *Aerosp. Sci. Technol.* **35**, 29 (2014).
- [2] A. H. Hosseinloo, S. P. Tan, F. F. Yap, and K. C. Toh, Shock and vibration protection of submerged jet impingement cooling systems: Theory and experiment, *Appl. Therm. Eng.* **73**, 1076 (2014).
- [3] A. H. Hosseinloo, F. F. Yap, and L. Y. Lim, Design and analysis of shock and random vibration isolation system for a discrete model of submerged jet impingement cooling system, *J. Vib. Control* **21**, 468 (2015).
- [4] A. H. Hosseinloo, F. F. Yap, and N. Vahdati, Analytical random vibration analysis of boundary-excited thin rectangular plates, *Int. J. Struct. Stab. Dyn.* **13**, 1250062 (2013).

- [5] M. F. Daqaq, R. Masana, A. Erturk, and D. D. Quinn, On the role of nonlinearities in vibratory energy harvesting: A critical review and discussion, *Appl. Mech. Rev.* **66**, 040801 (2014).
- [6] F. Cottone, H. Vocca, and L. Gammaitoni, Nonlinear Energy Harvesting, *Phys. Rev. Lett.* **102**, 080601 (2009).
- [7] A. Erturk and D. Inman, Broadband piezoelectric power generation on high-energy orbits of the bistable duffing oscillator with electromechanical coupling, *J. Sound Vib.* **330**, 2339 (2011).
- [8] M. A. Karami and D. J. Inman, Powering pacemakers from heartbeat vibrations using linear and nonlinear energy harvesters, *Appl. Phys. Lett.* **100**, 042901 (2012).
- [9] R. Harne and K. Wang, A review of the recent research on vibration energy harvesting via bistable systems, *Smart Mater. Struct.* **22**, 023001 (2013).
- [10] A. H. Hosseinloo and K. Turitsyn, Non-resonant energy harvesting via an adaptive bistable potential, *Smart Mater. Struct.* **25**, 015010 (2016).
- [11] K. Bergey, The Lanchester-Betz limit (energy conversion efficiency factor for windmills), *J. Energy* **3**, 382 (1979).
- [12] W. Shockley and H. J. Queisser, Detailed balance limit of efficiency of p - n junction solar cells, *J. Appl. Phys.* **32**, 510 (1961).
- [13] C. E. Shannon, Coding theorems for a discrete source with a fidelity criterion, *IRE Nat. Conv. Rec.* **4**, 1 (1959).
- [14] M. M. Seron, J. H. Braslavsky, and G. C. Goodwin, *Fundamental Limitations in Filtering and Control* (Springer-Verlag, London, 1997).
- [15] P. D. Mitcheson, T. C. Green, E. M. Yeatman, and A. S. Holmes, Architectures for vibration-driven micropower generators, *J. Microelectromech. Syst.* **13**, 429 (2004).
- [16] P. D. Mitcheson, E. M. Yeatman, G. K. Rao, A. S. Holmes, and T. C. Green, Energy harvesting from human and machine motion for wireless electronic devices, *Proc. IEEE* **96**, 1457 (2008).
- [17] R. Ramlan, M. Brennan, B. Mace, and I. Kovacic, Potential benefits of a non-linear stiffness in an energy harvesting device, *Nonlinear Dyn.* **59**, 545 (2010).
- [18] E. Halvorsen, C. P. Le, P. D. Mitcheson, and E. M. Yeatman, Architecture-independent power bound for vibration energy harvesters, *J. Phys. Conf. Ser.* **476**, 012026 (2013).
- [19] J. Heit and S. Roundy, A framework for determining the maximum theoretical power output for a given vibration energy, *J. Phys. Conf. Ser.* **557**, 012020 (2014).
- [20] E. Halvorsen, Fundamental issues in nonlinear wideband-vibration energy harvesting, *Phys. Rev. E* **87**, 042129 (2013).
- [21] R. Langley, A general mass law for broadband energy harvesting, *J. Sound Vib.* **333**, 927 (2014).
- [22] H. K. Joo and T. P. Sapsis, Performance measures for single-degree-of-freedom energy harvesters under stochastic excitation, *J. Sound Vib.* **333**, 4695 (2014).
- [23] C. Jarzynski, Nonequilibrium Equality for Free Energy Differences, *Phys. Rev. Lett.* **78**, 2690 (1997).
- [24] U. Seifert, Entropy Production along a Stochastic Trajectory and an Integral Fluctuation Theorem, *Phys. Rev. Lett.* **95**, 040602 (2005).
- [25] R. Chetrite and K. Gawdzki, Fluctuation relations for diffusion processes, *Commun. Math. Phys.* **282**, 469 (2008).
- [26] K. Turitsyn, M. Chertkov, V. Chernyak, and A. Puliafito, Statistics of Entropy Production in Linearized Stochastic Systems, *Phys. Rev. Lett.* **98**, 180603 (2007).
- [27] R. D. Astumian, Adiabatic operation of a molecular machine, *Proc. Natl. Acad. Sci. U.S.A.* **104**, 19715 (2007).
- [28] D. Abreu and U. Seifert, Extracting work from a single heat bath through feedback, *Europhys. Lett.* **94**, 10001 (2011).
- [29] H. Sandberg, J.-C. Delvenne, N. J. Newton, and S. K. Mitter, Maximum work extraction and implementation costs for nonequilibrium Maxwell's demons, *Phys. Rev. E* **90**, 042119 (2014).
- [30] V. Novikov, M. A. Shifman, A. Vainshtein, and V. I. Zakharov, Instanton effects in supersymmetric theories, *Nucl. Phys.* **B229**, 407 (1983).
- [31] G. Falkovich, I. Kolokolov, V. Lebedev, and A. Migdal, Instantons and intermittency, *Phys. Rev. E* **54**, 4896 (1996).
- [32] S. Boyd and L. Vandenberghe, *Convex Optimization* (Cambridge University Press, Cambridge, England, 2004).
- [33] P. L. Green, E. Papatheou, and N. D. Sims, Energy harvesting from human motion and bridge vibrations: An evaluation of current nonlinear energy harvesting solutions, *J. Intell. Mater. Syst. Struct.* **24**, 1494 (2013).
- [34] J. M. Kluger, Master's thesis, Massachusetts Institute of Technology, 2014.
- [35] G. Litak, M. Friswell, and S. Adhikari, Magnetopiezoelectric energy harvesting driven by random excitations, *Appl. Phys. Lett.* **96**, 214103 (2010).
- [36] T. Galchev, H. Kim, and K. Najafi, Micro power generator for harvesting low-frequency and nonperiodic vibrations, *J. Microelectromech. Syst.* **20**, 852 (2011).
- [37] P. Basset, D. Galayko, F. Cottone, R. Guillemet, E. Blokhina, F. Marty, and T. Bourouina, Electrostatic vibration energy harvester with combined effect of electrical nonlinearities and mechanical impact, *J. Micromech. Microeng.* **24**, 035001 (2014).